Journal of Minerals and Materials Characterization and Engineering, 2019, 7, 468-479
https://www.scirp.org/journal/jmmce
ISSN Online: 2327-4085
ISSN Print: 2327-4077

Bismuth Oxide Carbonate Structures Synthesized by Microwave—Assisted Solvothermal Approach and Its Use as Catalyst for the Degradation of Azo Dye in a Solution

M. A. Luna-Alvarado, M. Estrada-Flores*, M. E. Manríquez-Ramírez, C. M. Reza-San Germán

Departamento de Ingeniería Química Industrial, Escuela Superior de Ingeniería Química e Industrias Extractivas, Instituto Politécnico Nacional, Ciudad de México, México

Email: *mestradaf0400@ipn.mx

How to cite this paper: Luna-Alvarado, M.A., Estrada-Flores, M., Manríquez-Ramírez, M.E. and Germán, C.M.R.-S. (2019) Bismuth Oxide Carbonate Structures Synthesized by Microwave—Assisted Solvothermal Approach and Its Use as Catalyst for the Degradation of Azo Dye in a Solution. *Journal of Minerals and Materials Characterization and Engineering*, **7**, 468-479.
https://doi.org/10.4236/jmmce.2019.76033

Received: September 20, 2019
Accepted: November 26, 2019
Published: November 29, 2019

Abstract

Because the textile industry wastewater is polluted with azo dyes, and in order to improve a process of wastewater remediation, the synthesized sample was evaluated in the photocatalysis of methylene blue and compared with commercial Bi_2O_3 and anatase TiO_2. Structures of bismuth oxide carbonate ($Bi_2O_2CO_3$) were successfully synthesized using a solution at 0.03 M concentration of sodium bismuthate as precursor and ethylene glycol as dissolvent by solvothermal microwave-assisted approach. The semiconductor catalyst samples were characterized by X-ray diffraction (XDR), scanning electron microscope (SEM) and Brunauer-Emmett-Teller analysis (BET). The application of the synthesized sample as catalyst, obtained a 68% of degradation. This result is better than the commercial Bi_2O_3 and close to the anatase TiO_2 degradation. This sample shows a variation in the formula (with the presence of carbonates) but also shows an acceptable degradation percentage according to TiO_2 results, making $Bi_2O_2CO_3$ a possible substitute of TiO_2.

Keywords

Carbonate Bismuth Oxide, Photocatalysis, Microwave-Solvothermal Synthesis, Methylene Blue, Degradation

1. Introduction

At the present time, the excess of residual liquids has become in a critical problem. There are a lot of pollutants in the water, among which are colorants and chemical substances. Industrial activities are significant contributors to the

wastewater pollution of all the water sources in the world, different industries, among which is textile as one of the largest generators of wastewater due to the dyeing and finishing process, where azo dyes are used [1]. There are a lot of attractive approaches that has been used as treatment for this wastewater. Heterogeneous photocatalysis is an advanced oxidation process widely used to the degradation of organic pollutants in water. It used semiconductors as catalyst for this process, normally. TiO_2 powder is employed for this purpose, however, different and economical materials as Bi_2O_3 have been studied to be used as substitute or complementary system [2].

On the other hand, the most used catalyst is titanium dioxide, TiO_2, which has proved that is highly efficient in degradation process of organic materials due to photocatalytic and photoconductor properties. This material has a band gap of 3.2 eV, which means that all UV radiation during a wavelength of 387 nm or less will have enough energy to turn on the catalyst [3]. It also has interesting properties such as transparency in visible light, refractive index, and low absorption coefficient [4]. Titanium dioxide has three different polymorphic structures: rutile (tetragonal), anatase (tetragonal) and brookite (orthorhombic). Also, it is a semi-conductor, usually during its anatase and rutile phase [5].

There have been many researches to know bismuth oxide's physicochemical properties. As a result, there is known that bismuth oxide has different structures which can be obtained with micro and nanometric structures. Besides this polymorphic characteristic, bismuth oxide is characterized for being a well ionic conductor because its band gap is between 2.7 - 2.8 eV and, it has a good photoconductivity [6].

Bismuth (III) oxide is one of the simplest oxides and it has the advantage of being economical and environmentally friendly. Nowadays, this oxide is used in different areas such as medicine and engineering, and also is used in cosmetics because of its low toxicity and, in the last few years, 43% of the bismuth production has been used as a replacement of lead [7].

According to several researches, this oxide has six polymorphic structures, yet, four of them are the most common: α, β, γ, δ, which two of them are stable; monocyclic phase α works at low temperatures and, cubic phase δ works at high temperatures, approximately at 1003.15 K; this phase is known because of its high ionic conductivity as oxide ions can move from side to side along bismuth arrangement. The other two intermediate meta-stables phases: tetragonal phase β occurs at 923.15 K and, the γ phase has a body centered cubic structure which is formed at 913.15 K [8].

In terms of this research, Mexico has maintained its second place in bismuth's world production with a maximum quantity of 1000 ton in 2010 [9], so bismuth oxide can replace titanium dioxide as catalyst.

For this research, α stable structure of bismuth oxide carbonate was used. It has parallel layers of bismuth atoms that are separated by layers of oxide ions. This allows the structure to have better superficial area. Also, due to low fusion point of bismuth, most of the methods that are used to synthesize different

structures do not apply to bismuth. Bismuth oxide carbonate was synthesized via solvothermal; however, to avoid long reaction periods, the experiment was microwave-assisted, which produces nanoparticles with low size dispersion, although is hard to have control on morphology. This technique has been used during the last few years as an alternative method to synthesize materials at a nanometric scale because it is a fast and effective method that allows to get more quantity of product in a short period of time [10]. The synthesized material was tested as catalyst of heterogeneous photocatalysis in the reaction of degradation of methylene blue, as azo dye used in many textile industries.

2. Experimental Procedure

2.1. Preparation of the $Bi_2O_2CO_3$ Catalyst

$BiNaO_3$ (Sigma Aldrich) was dissolved in ethylene glycol (Reasol) to produce a 0.03M solution and maintained continuous stirring at 700 rpm for 15 min, then, the resulting solution was transferred into a digestion vessel (Parr mod. 4781). After that, the vessel was introduced into a microwave oven (Amana Commercial Mod. HDC12A2), the solution was irradiated at 1200 Watts for 10 seconds. Finally, the precipitates were centrifuged and washed several times using distilled water and isopropyl alcohol intercalary. The resulting precipitates were dried for 1 h in an oven (Neytech Qex mod. V1.2) at 100˚C for 1 hour.

2.2. Characterization Details

The surface morphology of the samples of commercial Bi_2O_3, $Bi_2O_2CO_3$ synthesized and commercial TiO_2 was characterized by scanning electron microscopy (SEM) in a JEOL microscope model JSM-7800F, with a resolution of 0.8 nm at 15 kV of acceleration in secondary electrons mode. A Rigaku diffractometer, model Miniflex 600 with X ray tube with Cu Ka (l = 1.54 A˚) radiation and lineal focus was used for XRD, with 40 kV y 15 mA. Symmetric measurements from 3 to 70 degrees with step of 0.01 and a speed or 3 degrees/minute. Nitrogen adsorption and desorption isotherms were measured at 77 K using Quantachrome Autosorb 1. Prior to the measurements, the Bi_2O_3 0.03 M and TiO_2 samples were outgassed at 100˚C for 25 h. and the commercial Bi_2O_3 sample was outgassed as the same temperature like the previous samples for 43 h. The specific surface area and the pore size distribution (average pore diameter and mean pore volume) were measured from the adsorption isotherm using the Brunauer-Emmett-Teller method and Barrett-Joyner-Halenda method, respectively.

2.3. Degradation of Methylene Blue

To verify the degradation of methylene blue ($C_{16}H_{18}ClN_3S$), it was prepared a 25-ppm solution (Sigma Aldrich). First a photolysis was made using 50 ml of the 25-ppm solution that was transferred to a quartz reactor. To make this experiment it was used a closed equipment that contained 8 UV lamps (50 W), and the solution was stirred at 600 rpm. During irradiation, 5 ml of the solution was re-

moved every 10 min for 2 h and went back inside the solution after being analyzed using a Perkin Elmer spectrophotometer 365 in a range of 400 - 700 nm to measure the absorbance of each sample. The commercial Bi_2O_3, synthesized $Bi_2O_2CO_3$ and TiO_2 catalyst were also studied under the same conditions.

3. Results and Discussion

3.1. DRX and SEM Analysis

The morphology of the samples was observed by SEM. **Figure 1(a)** shows the surface of the synthesized Bi_2O_3 sample composed by agglomerated foils of 5 μm maximum that might have very good results in photocatalytic activity because of the porosity found on the structure. These foils started to grow during the first 10 seconds of irradiation. The next two images are from the commercial Bi_2O_3 (**Figure 1(b)**) and TiO_2 (**Figure 1(c)**) respectively, these structures show difference between morphology and how it affects the degradation of methylene blue because the images show that TiO_2 particles are sphere shaped with an average diameter between 100 to 200 nm, while Bi_2O_3 shows compact agglomerate structures with a diameter of 10 μm.

According to diffraction pattern, **Figure 1(a)** corresponds to a body centered tetragonal crystalline structure with unit cell parameters a = b = 3.865 and c = 13.675 and angles of α. β, γ de 90˚, this information matches accurately to the crystallographic PDF chart 41-1488, of the bismuth oxide carbonate ($Bi_2O_2CO_3$). **Figure 1(b)** shows the diffraction pattern of the alpha bismuth oxide (Bi_2O_3), where the corresponding PDF chart is 71-0465 and demonstrated the presence of a monoclinic system with space group P-21/c(14) and lattice parameters of a = 5.849, b = 8.164 and c = 7.510 and the angle β = 112.97. Finally, **Figure 1(c)** show the XRD of commercial TiO_2 anatase phase agree with the PDF chart 89-4921 where tetragonal system is reported with lattice parameters of a = b = 3.77 and c = 9.501, angles of 90˚ and space group I41/ad(141).

3.2. Nitrogen Adsorption - Desorption Measurements

The nitrogen adsorption-desorption isotherms of TiO_2 and Bi_2O_3 structures are shown in **Figure 2**. The TiO_2 and synthesized Bi_2O_3 are a type II isotherm curves. It is observed that the synthesized Bi_2O_3 adsorbed better the N_2 due to a bigger surface area and pore radius. The commercial Bi_2O_3 is a type III isotherm due to the small surface area and pore volume in comparison to the other isotherms.

The corresponding average pore diameter and total pore volume are calculated from the BJH pore size distribution curves and the values are given in **Table 1**, it is clear that the molecules synthesized of $Bi_2O_2CO_3$ exhibit a superior surface area and also a higher pore diameter and pore volume than TiO_2 particles. The commercial Bi_2O_3 surface area is 5.64 times smaller than the synthesized sample and it is because a precursor solution with low concentration was used for the synthesis and also the small period of time on the microwave affected positively the porosity of the structure. The specific surface area for the

$Bi_2O_2CO_3$, Bi_2O_3 and TiO_2 materials is also listed in Table 1.

3.3. Optical Properties

The band gap energy was measured using a Perkin Elmer spectrophotometer 365 with integration sphere at wavelength of 500 to 300 nm in Absorbance mode. The Kubelka-Munk method was used to determine the band gap energy. According to the Kubelka-Munk method the Equation (1) was be used:

Table 1. Surface area, total pore volume, and average pore diameter of commercial Bi_2O_3, anatase TiO_2 and synthesized $Bi_2O_2CO_3$.

Sample	Surface area (m^2/g)	Total pore volume (cm^3/g)	Average pore radius (Å)
$Bi_2O_2CO_3$	25.03	0.1209	90.37
Commercial Bi_2O_3	4.435	0.006006	21.04
Anatase TiO_2	9.819	0.2302	67.4

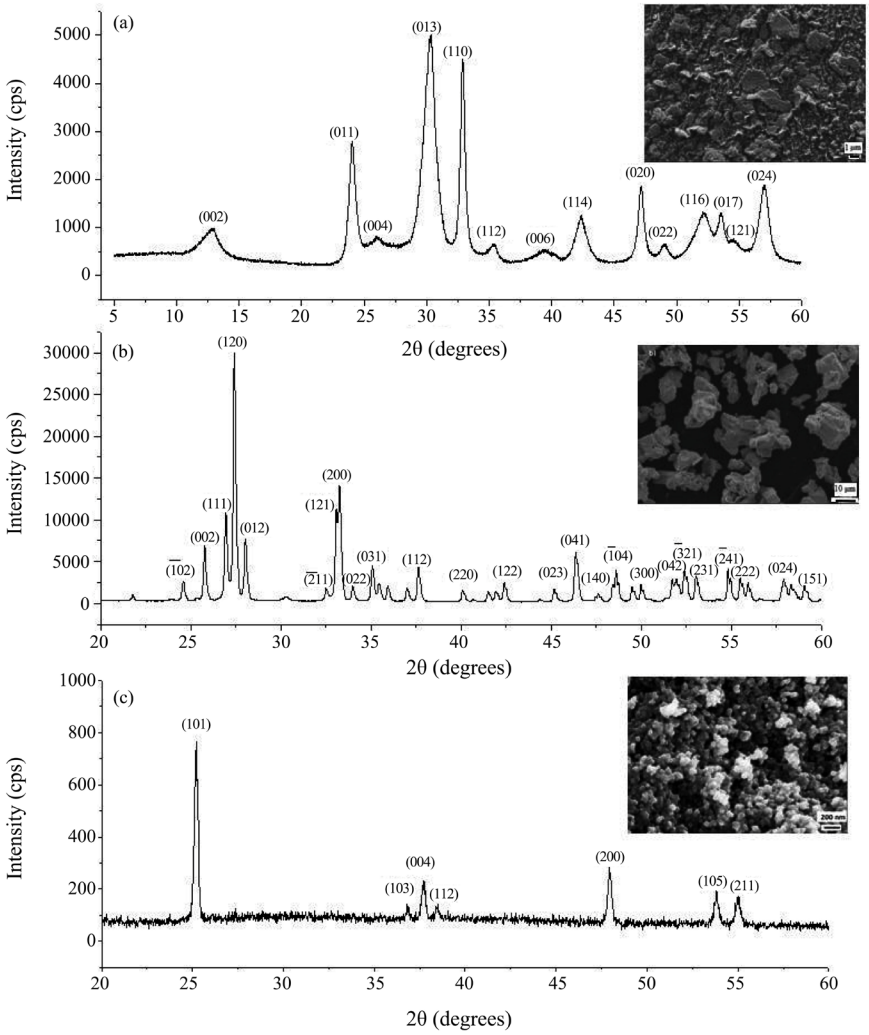

Figure 1. XDR and SEM micrograph of (a) Synthesized $Bi_2O_2CO_3$, (b) commercial Bi_2O_3, (c) commercial TiO_2.

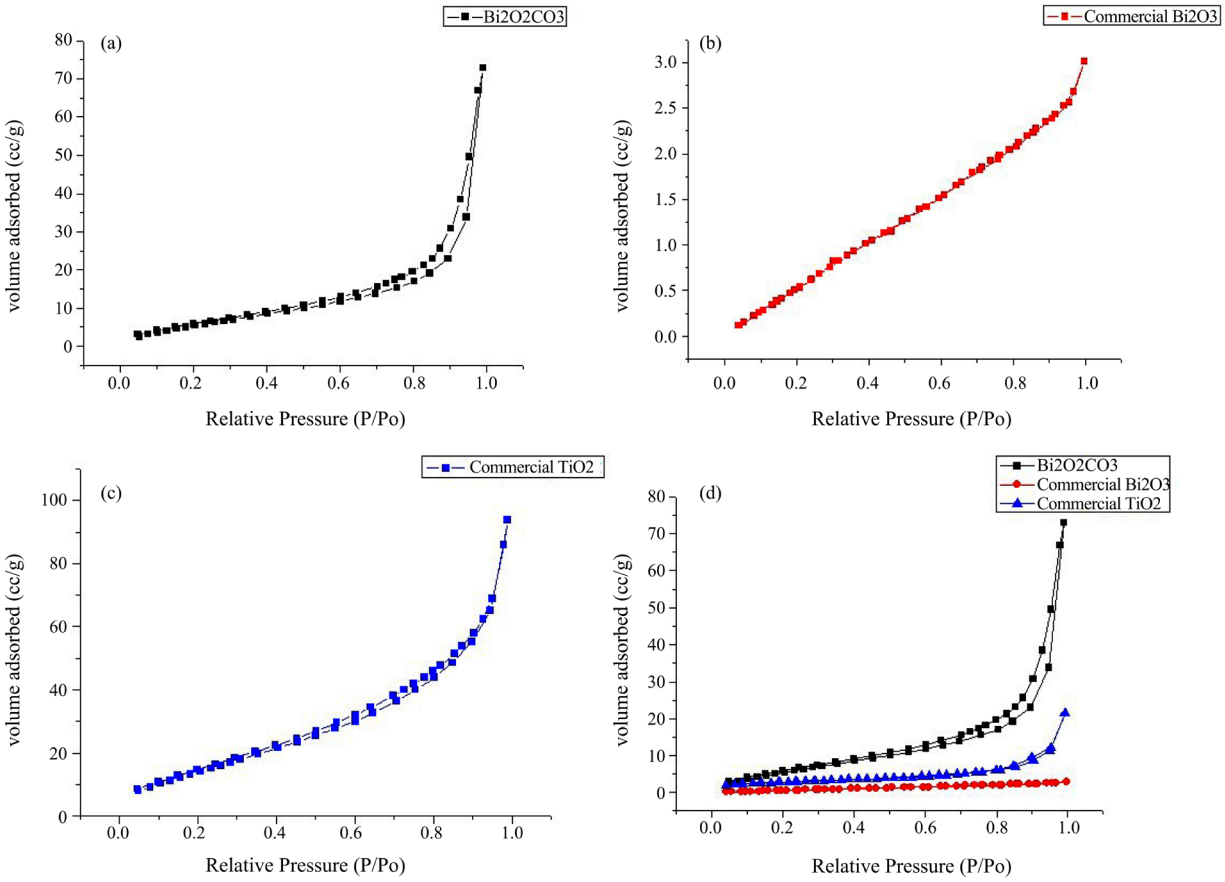

Figure 2. N_2 adsorption-desorption isotherms, (a) $Bi_2O_2CO_3$, (b) commercial Bi_2O_3, (c) commercial TiO_2, (d) isotherm comparison.

$$(\alpha h\upsilon)^n = A(h\upsilon - E_g) \tag{1}$$

where α, υ, A, E_g are the absorption coefficient, light frequency, a constant and the band gap energy, the n is determined by the type of optical transition in the semiconductor (*i.e.* n = 2 for the direct transition and n = 1/2 for the indirect transition). Taking in consideration that the samples are an indirect semiconductor, the band gap energy is determined from a plot of $(\alpha h\upsilon)^{\frac{1}{2}}$ vs. Band gap energy, obtaining the results shown in Table 2.

As it can be observed, the value of $Bi_2O_2CO_3$ band gap is inside the range of the theoretical values which supports the theory that it is actual $Bi_2O_2CO_3$ and not another compound, and because of its higher value, it needs more energy than anatase, that is one of the reasons that degradation percentage is slower than anatase.

3.4. Kinetics of Degradation of Methylene Blue

The degradation of methylene blue is until the final stage of the process shown in Figure 3, give as result the formation of CO_2 and water, removing the dye in the original solution. In this work, we follow the reaction only with the dye concentration respect the time.

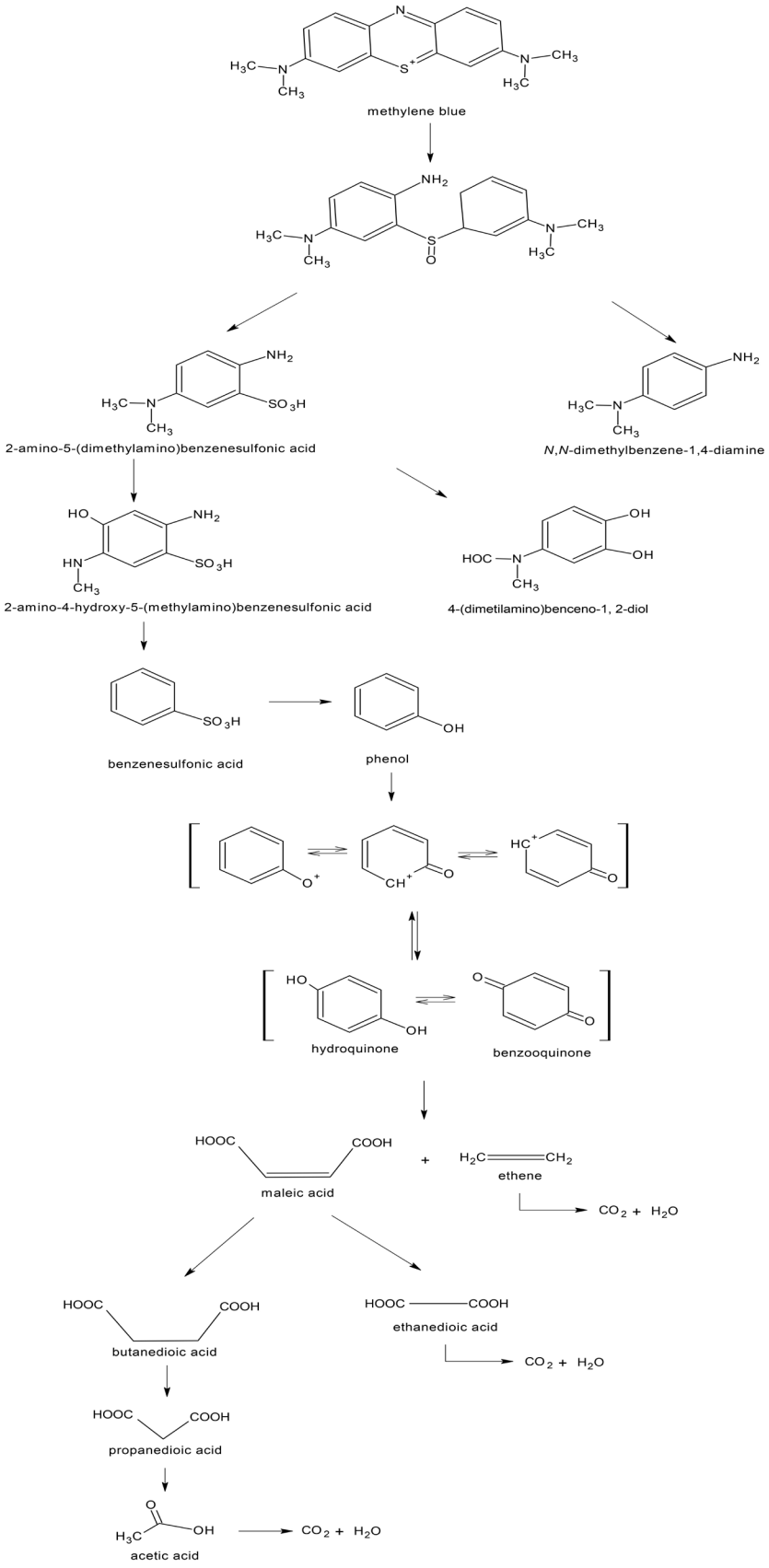

Figure 3. Degradation process of the methylene blue [16].

Table 2. Band gap data obtained from the Kubelka-Munk method and the theorical ones.

Band gap	$Bi_2O_2CO_3$	Commercial Bi_2O_3	Anatase TiO_2
Measured	3.35 eV	2.6 eV	3.0 eV
Theorical	2.25 - 3.55 eV [11] [12]	2.7 - 2.9 eV [6] [13]	2.86 - 3.34 eV [14] [15]

The experimental section of the application was carry out following the next procedure: first a calibration curve was obtained, in order to know the concentration of dye in the solution, a photolysis to know the degradation caused by the lamps and finally, the three catalyst were proved at the same conditions.

The calibration curve of methylene blue was obtained to calculate the concentration of the solutions in relation to time. It is clearly observed that the adjusted R-squared value is equal to 0.99756, with an adjusted equation $y = 0.1103x - 0.01103$. This data allows to obtain the concentration of each sample of methylene blue solutions that were taken during the degradation experiments.

To obtain the data for **Table 3** some equations were used. Langmuir-Hinshelwood was employed to obtain the first approximation, considering a first order kinetics, as is used in organic dyes in low concentrations. The different concentrations of each solution were calculated using the adjusted equation of the calibration curve (Equation (2)).

$$C_{MB} = \frac{Abs + 0.1148}{0.1148} \tag{2}$$

The equation above needs the Absorbance in different time (Abs), and the result is the concentration of methylene blue in the solution (C_{MBS}). Then, the percentage of methylene blue in solution was calculated in order to obtain the degradation efficiency, the Equation (3) was used

$$\%C_{MB} = \frac{MB_S * 100}{C_0} \tag{3}$$

C_O is the initial concentration of each experiment and finally, the degradation efficiency of each catalyst was calculated by the Equation (4):

$$\%D_{MB} = 100 - \%MB_S \tag{4}$$

where D_{MB} is the degradation efficiency of catalysts and MBs is the percentage of methylene blue in solution. The table below shows the degraded methylene blue percentage in relation to time.

Figure 4 shows the comparison of the different experiments to show the degradation percentage of the methylene blue along the 120 min. TiO_2 degrades 85.64% of the solution while $Bi_2O_2CO_3$ shows a degradation percentage of 68.25, showing that the morphology affects positively on the photocatalytic activity. Morphology plays an important role in photocatalytic activity because commercial Bi_2O_3 is formed by agglomerated compacted structure that reduces its surface area. A serial of factors influence the photocatalytic reaction with Bi_2O_3, among which are: due to its hybridation (Bi 6s and O 2p orbital), it is a strong oxidizer and can successfully degrade organic compounds and favors the mobility of photoholes in the valence band [17].

Table 3. Degraded methylene blue percentage.

Time (min)	Photolysis	$Bi_2O_2CO_3$	Commercial Bi_2O_3	Anatase TiO_2
0	0	0	0	0
10	10.4679	60.2842	29.5348	14.3705
20	10.7898	62.8541	30.0239	26.1621
30	10.8316	63.2387	30.1803	35.4951
40	10.8339	64.4867	31.4892	41.4745
50	10.8674	65.2364	36.2470	47.9653
60	11.0419	65.2746	38.0888	55.4298
70	11.1100	65.7818	38.9539	63.9367
80	11.3709	66.6508	40.2249	71.1749
90	11.5032	67.7182	40.2810	77.5477
100	11.6802	67.9340	41.4341	80.2620
110	20.2549	68.1760	42.9989	82.5338
120	24.7961	68.2573	50.3846	85.6415

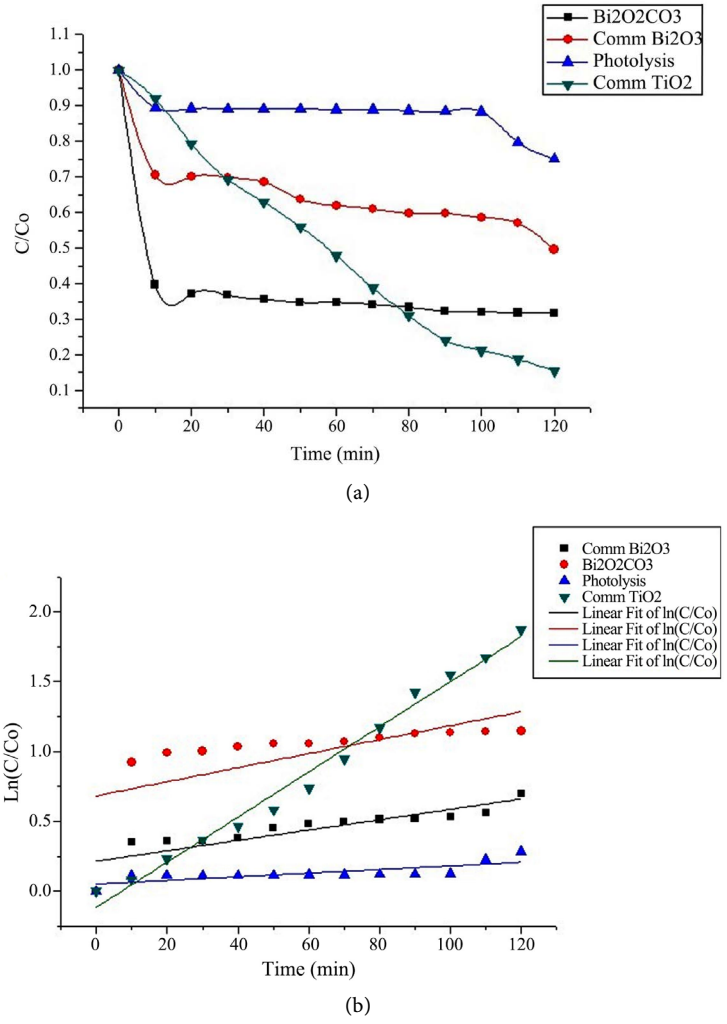

Figure 4. Degradation curves of methylene blue.

According to Levenspiel, the equation used to get the parameters come from the reaction rate equation in terms of the concentration of the reactant

$$-r_A = -\frac{dC_A}{dt} = kC_A^n \tag{5}$$

where n means the order of the reaction, k is the rate constant and the C_A is the concentration of the reactant, which in this case is methylene blue.

It is well known that the concentration of the reactants in time t can be explained by the Equation (6)

$$C_A = C_{A0}\left(1 - X_A\right) \tag{6}$$

C_{A0} is the initial concentration of the catalyst and X_A is the degree of conversion of the reactant. Then, the substitution of Equation (6) in Equation (5) is next

$$-r_A = C_{A0}\frac{dX_A}{dt} = k\left(C_{A0}\left(1 - X_A\right)\right)^n \tag{7}$$

Knowing the time of the experiment, the change of concentration in time t due to absorbance measurement and the initial concentration of each experiment, the equation to know the rate constant is shown below as Equation (8).

$$k = \frac{1}{t}\int_0^{X_A} \frac{dX_A}{{C_{A0}}^{n-1}\left(1 - X_A\right)^n} \tag{8}$$

Table 4 shows the results of the calculus made to get the approximately kinetic constant of each catalyst and to understand their behavior during the photocatalysis. Even that they are first order kinetics, the speed constant of $Bi_2O_2CO_3$ shows a bigger constant than TiO_2 Anatase because during the first 20 minutes of UV radiation, $Bi_2O_2CO_3$ degrades better than TiO_2. The same behavior is shown with Commercial Bi_2O_3. For the experiment anatase TiO_2 was used because its properties are well known, the superficial area has a value of 10 - 17 m^2/g [18] [19]. TiO_2 anatase band gap experimental value is 3.0 eV which shows that needs more energy to get excited and to degrade in a higher way.

Table 4. Kinetic parameters of the catalysts used.

	Photolysis	$Bi_2O_2CO_3$	Commercial Bi_2O_3	Anatase TiO_2
k (rate constant) [min^{-1}]	0.0031 min^{-1}	0.01310 min^{-1}	0.0105 min^{-1}	0.02606 min^{-1}
Kinetic model	$-r_{MB} = 0.0031\ C_{MB}$	$-r_{MB} = 0.0131\ C_{MB}$	$-r_{MB} = 0.0105\ C_{MB}$	$-r_{MB} = 0.02606\ C_{MB}$

4. Conclusions

Anatase TiO_2 clearly has the highest degradation percentage of all samples. However, the Bi_2O_3 structure that was synthesized by solvothermal method using microwave irradiation shows a variation in the formula indicating traces of CO_3 but also shows an acceptable degradation percentage according to TiO_2 results, making $Bi_2O_2CO_3$ a possible substitution of TiO_2. It needs to be mentioned

that BET area shows that $Bi_2O_2CO_3$ is clearly superior than Anatase TiO_2 including pore radius. This will indicate in the future that with the proper conditions, it can degrade better than TiO_2. Also, the morphology highly affects degradation process: if the structure possesses high porosity, it will have a high degradation percentage. In terms of band gap, the experimental value of $Bi_2O_2CO_3$ is inside of theoretical values, but the amount of energy needed in the degradation experiment is higher than anatase; that is one of the principal reasons why anatase has a higher degradation percentage, however, $Bi_2O_2CO_3$ presents acceptable results, especially in the first minutes of reaction. It is important to consider that Mexico has the second place in bismuth oxide production worldwide, and this allows to reduce costs and to get the catalyst inside the country. Wastewater problem could be decreased considerably using a system like the presented in this research.

Acknowledgements

Authors are thankful to IPN for the support to SIP projects: 20196017, 20190616 and 20190251.

Conflicts of Interest

The authors declare no conflicts of interest regarding the publication of this paper.

References

[1] Estrada, M., Reza, C., Salmones, J., Wang, J.A., Manríquez, M.E., Mora, J.M., Hernández, M.L., Zúñiga, A. and Contreras, J.L. (2014) Synthesis of Nanoporous tio2 Thin Films for Photocatalytic Degradation of Methylene Blue. *Journal of New Materials for Electrochemical Systems*, **17**, 23-28. https://doi.org/10.14447/jnmes.v17i1.439

[2] Singh, R.P., Singh, P.K., Gupta, R. and Singh, R.L. (2019) Treatment and Recycling of Wastewater from Textile Industry. Advances in Biological Treatment of Industrial Waste Water and their Recycling for a Sustainable Future. Applied Environmental Science and Engineering for a Sustainable Future. Springer, Singapore. https://doi.org/10.1007/978-981-13-1468-1_8

[3] Hernández, J., García Serrano, L., Zeifert, B., García, R., Zermeño, B., Del Ángel, T. and Cueto, H. (2008) Synthesis and Characterization of N-TiO_2-Anatase Nanoparticles. *Mexican Society of Science and Surfaces and Materials Technology*, **21**, 1-5.

[4] Ibáñez, P. (2003) Colloidal Properties of TiO_2 Particles: Application to the Solar Photocatalytic Water Treatment. Granada's University, Granada, 27-33.

[5] Maimone, A., Camero, S. and Blanco, S. (2015) Characterization of Titanium Dioxide Obtained by Thermal Treatment and Electrochemical Anodization. *Engineering School's Magazine U.C.V.*, **30**, 189-200.

[6] Otálora, D., Orozco, G. and Olaya-Flórez, J. (2015) Microstructure and Optical Properties of Bismuth and Bismuth Oxide Films by Unbalanced Magnetron Sputter Deposition. *Magazine of the Colombian Academy of Exact, Physical and Natural Sciences*, **39**, 18-25.

[7] INEGI (2014) Mexico's Mining in 2014. Sector Statistics.

[8] Otálora, D. (2011) Study of Electrical and Optical Properties of Nanostructured of Bismuth and Bismuth Oxide Coating. Colombia's National University, Bogotá, 18-22.

[9] Osorio, M. (2011) Synthesis and Characterization of Monolayer Nanotubes, Multilayer Nanotubes and Bismuth Nanoparticles Obtained by Microwave Irradiation. Nuevo Leon University, Monterrey City, Mexico, 12-37.

[10] De León, I. (2014) Bismuth Oxide: The Effect of l-Lysine in Physicochemical and Photocatalytic Properties of Bismuth Oxide Synthesized by Sonoprecipitation. Nuevo Leon University, Monterrey City, Mexico, 28-30.

[11] Lian, Y., Ying, L., Li, C. and Wang, H. (2017) Improved Photocatalytic Properties of Flower-Like $Bi_2O_2CO_3/TiO_2$ Nanocomposite Structures. *Digest Journal of Nanomaterials and Biostructures*, **12**, 1107-1117.

[12] Chen, L., *et al.* (2012) $Bi_2O_2CO_3$/BiOI Photocatalysts with Heterojunctions Highly Efficient for Visible-Light Treatment of Dye-Containing Wastewater. *Industrial and Engineering Chemistry Research*, **51**, 6760-6768. https://doi.org/10.1021/ie300567y

[13] Gadhi, T., Hernandez, A., Bizarro, M., Jagdale, P., Tagliaferro, A. and Rodil, S. (2016) Efficient a/b-Bi_2O_3 Composite for the Sequential Photodegradation of Two-Dyes Mixture. *Ceramics International*, **42**, 13065-13073. https://doi.org/10.1016/j.ceramint.2016.05.087

[14] Valencia, S., Marin, J. and Restrepo, G. (2010) Study of the Bandgap of Synthesized Titanium Dioxide Nanoparticles Using the Sol-Gel Method and a Hydrothermal Treatment. *The Open Materials Science Journal*, **4**, 9-14. https://doi.org/10.2174/1874088X01004020009

[15] Hossain, F., Sheppard, L., Nowotny, J. and Murch, G. (2005) Optical Properties of Anatase and Rutile Titanium Dioxide: *Ab Initio* Calculations for Pure and Anion-Doped Material. *Journal of Physics and Chemistry Solids*, **69**, 1820-1828. https://doi.org/10.1016/j.jpcs.2008.01.017

[16] Miriam, E.F. (2011) Síntesis, caracterización estructural y evaluación fotocatalítica de películas de alúmina—titania. Instituto Politécnico Nacional. 96-97.

[17] Zhang, L.S., Wang, W.Z., Yang, J., Chen, Z.G., Zhang, W.Q., Zhou, L. and Liu, S.W. (2006) Sonochemical Synthesis of Nanocrystallite Bi_2O_3 as a Visible-Light-Driven Photocatalyst. *Applied Catalysis A*: *General*, **308**, 105-110. https://doi.org/10.1016/j.apcata.2006.04.016

[18] Hussain, M., Ceccarelli, R., Marchisio, D., Fino, D., Russo, N. and Geobaldo, F. (2010) Synthesis, Characterization, and Photocatalytic Application of Novel TiO_2 Nanoparticles. *Chemical Engineering Journal*, **157**, 45-51. https://doi.org/10.1016/j.cej.2009.10.043

[19] Kang, J., Lim, J., Rho, W. and Kim, J. (2016) Wrinkled Silica/Titania Nanoparticles with Tunable Interwrinkle Distances for Efficient Utilization of Photons in Dye-Sensitized Solar Cells. *Scientific Reports*, **6**, Article No. 30829. https://doi.org/10.1038/srep30829